

Actin-Myosin Interaction

Structural model: Both F-actin and myosin are large protein molecules whose interaction takes place at multiple sites in a very specific manner. From the independent X-ray structure of G-actin (Fig. A5) and S1 (Fig. M8) and from electron density maps of actin filaments decorated with S1, the three-dimensional structure of actoS1 was reconstructed as shown on Fig. AM1.

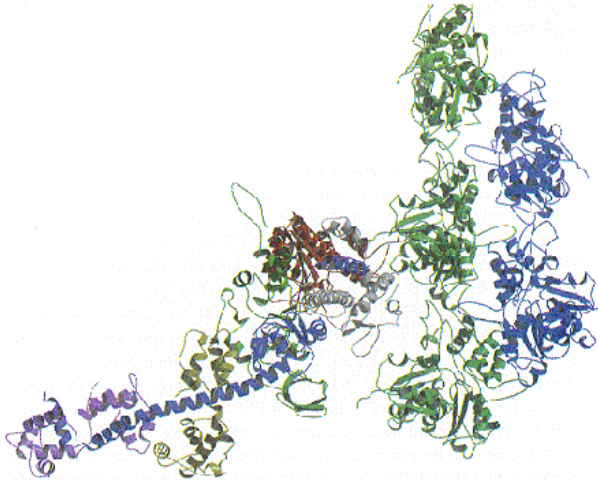


Fig. AM1. Three-dimensional atomic model of F-actin combined with myosin subfragment 1. (From Geeves and Holmes, with permission from the Annual Review of Biochemistry, vol. 68, pp. 687-728, 1999, Copyright by Annual Reviews, <http://www.AnnualReviews.org>). Ribbon representation of the myosin-actin interaction. The ribbon on the left corresponds to myosin subfragment 1; an F-actin double helix consisting of 5 actin globules is shown on the right.

Contact sites: As discussed in connection with Fig. A5, the G-actin molecule has four subdomains, most of the amino acids that are involved in the interaction with S1 are located in its subdomain 1.

As discussed in connection with the three-dimensional structure of S1, the first helix of the 20-kDa fragment and the lower and upper domains of the 50-kDa fragment contain the actin-binding site of S1.

The first contact involves positively charged lysine residues of S1, at the 20-50-kDa junction, and negatively charged amino acid residues of actin subdomain 1 (Furch et al., 2000). This is a non-specific electrostatic contact; it constitutes the weak binding between S1 and actin.

The second contact involves hydrophobic residues of both S1 and actin. This is a stereospecific interaction. The lower domain of the 50-kDa fragment of S1 is linked to residues mainly from subdomain 1 of actin and a few from subdomain 3.

The third contact strengthens the second one by recruitment of additional loops from the upper domain of the 50-kDa fragment of S1 and subdomain 2 of actin. This interaction follows the cleft closure between the lower and upper domains of the 50-kDa fragment of S1.

The formation of tightly bound state from the weakly bound state occurs with the second and third contacts. Strong binding is necessary for the power stroke.

Arginine 405, participating in the third contact, is a conserved amino acid residue in all studied myosins. It is functionally important; namely, it was demonstrated that mutation of arginine 405 to glutamine is one cause of familial hypertrophic cardiomyopathy.

These three contacts involve a single actin subunit and define the primary site of actin-myosin interaction. In addition, the model building brings a second region of S1 into the proximity of the neighboring actin monomer, one helix turn below. The main contribution to this secondary interaction with actin comes from a loop that corresponds to residues 567-578 in the S1 sequence.

Remarkable functional conservation is found in the way in which actin and myosin isoforms from different species interact. Such findings suggest a constancy of the structure of the molecular contacts at the actomyosin interface.

Recent advances in this field include molecular engineering of myosin (Manstein, 2004). A series of mutant constructs in which the charge and length of S1 loop 2 were changed revealed a correlation between the charge of the loop, the activation by actin of the mutant constructs ATPase rates, and the strength of the interaction between mutant motor domain and actin. The addition of 4 to 12 positive charges to loop 2 increased the affinity for actin up to 120-fold, V_{\max} up to 5-fold, and the efficiency of coupling between the actin and nucleotide binding sites 30-70-fold.

A spectacular achievement of the myosin engineering is the backward-moving myosin motor (reviewed by Manstein, 2004).

Lever Arm Model

The current hypothesis for the mechanism of force generation by actin-myosin-ATP postulates the rotation of the lever arm as the primary mechanical component of the power stroke. The lever arm is an 85Å-long alpha helix, to which the regulatory and essential myosin light chains are bound. During the ATP-binding and subsequent ATP-hydrolysis, the active site area of subfragment 1 undergoes subtle conformational changes and as a result the lever arm moves through 11 nm along the actin helix axis (Figs. AM1a and AM1b). There are several reports which suggest that the length of the lever arm is proportional to the step-size of the movement. On other hand, the latest report indicates that different myosins may have different step-sizes for the same length of the lever arm (reviewed by Geeves and Holmes, 2005). The rotation of the lever arm (Dominguez et al., 1998) that is thought to occur during force production is illustrated in Fig. AM1c.

Rotation of the lever arm in contracting skeletal muscle fiber was also shown by two-photon anisotropy (Borejdo et al., 2004).

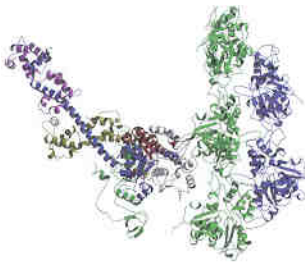


Fig. AM1a. Illustration of the lever arm's position in the pre-power-stroke state of actomyosin (From Geeves and Holmes with permission from the Annual Review of Biochemistry, vol. 68, 1999, Copyright by Annual Reviews, <http://www.AnnualReviews.org>). Five different actin monomers in two strands of the actin double helix are shown *right*, a myosin cross-bridge (S1 in Fig. M8) is shown *left*.

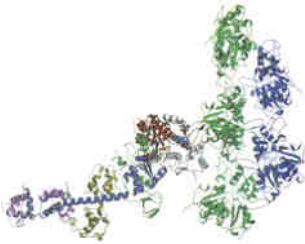


Fig. AM1b. Illustration of the lever arm's position in the post-power-stroke state of actomyosin (From Geeves and Holmes with permission from the Annual Review of Biochemistry, vol. 68, 1999, Copyright by Annual Reviews, <http://www.AnnualReviews.org>).

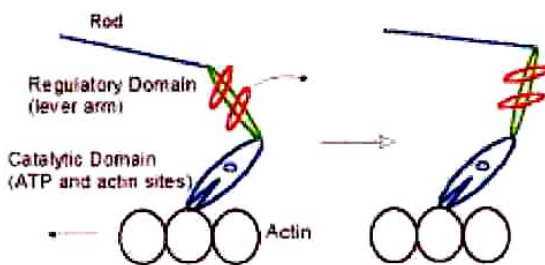


Fig. AM1c. Illustration of the rotation of the lever arm during force production (From Highsmith, reprinted with permission from Biochemistry, 38, 791-797, 1999, Copyright 1999, American Chemical Society).

An important feature of the lever arm model is that it has the myosin light chain domain rigidly attached to the converter domain and not by a mobile joint. Converter and lever arm swing together in a rigid body motion with its axis of rotation close and almost parallel to the relay helix. Other important parts of the S1 structure are: The cleft, which separates the upper 50K and the lower 50K domains; both domains are involved in actin-binding. The ATP-binding site, which lies close to the apex of the cleft contains the P-loop motif flanked by the switch 1 (SW1) and switch 2 (SW2) segments. SW2, which is structurally part of the lower 50K domain, connects with the relay helix.

Dynamics of actin-myosin interaction: The primary goal of studies on actin-myosin interactions is to identify the conformations of the myosin crossbridges associated with the Lymn and Taylor cycle (1971). A large variation of approaches are used: Conibear et al., (2003) monitored myosin cleft movement using pyrene excimer fluorescence from probes engineered across the cleft. Structural studies have indicated that communication between the actin- and nucleotide-binding sites involves the opening and closing of the cleft between the upper and lower 50K domains of myosin-S1. That is the movement of SW1 toward its closed state (where it contacts the nucleotide through the Mg^{2+} and γ -phosphate); this movement is accompanied by opening of the myosin cleft and weakening of the actin binding site. Furthermore, MgADP provides less of a driving

force toward the cleft open state and hence gives a more limited and slower dissociation of actin as compared with MgATP, which strongly favors cleft opening. .

The dynamics of actomyosin interactions in relation to the crossbridge cycle was investigated by Zeng et al. (2004). Probes have been introduced in the *Dicytostelium* myosin II motor domain via three routes: 1) single tryptophan residues at strategic locations throughout the motor domain; 2) green fluorescent protein fusions at the N and C termini; and 3) labeled cysteine residues across the actin-binding cleft. These studies suggested that the tryptophan in the relay loop senses the lever arm position which is controlled by SW2 open-to-closed transition at the active site. Actin has little effect on this process. SW1 closing appears to be a key step in the nucleotide induced actin dissociation, while its opening is required for the subsequent activation of product release.

Reubold et al. (2003) presented a structural model for actin-induced nucleotide release in myosin. These authors have crystallized the nucleotide-free motor domain of myosin II in a new conformation in which SW1 and SW2 conserved loop structures involved in nucleotide binding, have moved away from the nucleotide binding pocket. These movements are linked to rearrangement of the actin-binding region, which illuminate a previously unobserved communication pathway between the nucleotide-binding pocket and the actin binding region, and explain the reciprocal relationship between actin and nucleotide affinity. Based on these results, authors have presented a potential scheme for the myosin cycle: In the transition-state structure both SW1 and SW2 are in the closed position (C/C0, phosphate release is blocked and the lever arm is in the up position. Hydrolysis of ATP leads to destabilization of the C/C state, The equilibrium between C/C and O/C (SW1 opened but SW2 is closed) is further shifted toward the O/C conformation by actin-binding. Weak association with actin induces a rearrangement of the actin-binding interface, resulting in full opening of SW1. This breaks the salt bridge between Arg238 and Glu 459, and accelerates P_i release through a newly formed “trapdoor”. Loss of P_i disrupts the hydrogen bond between the SW2 glycine and the γ -phosphate, thereby allowing SW2 to open, leading to ADP release.

Dynamic docking of myosin and actin observed with resonance energy transfer (Root et al., 2002) suggest that the larger movements in the light chain binding domain are accompanied by twisting and rotating movements of the catalytic domain, causing a tilt of approximately 30° during the weak-to-strong transition of the actin-myosin binding.

Physiologically important reports about the nature of the actin-myosin interaction are; Phosphate release is the rate limiting step in the overall ATPase of psoas myofibrils (Lionne et al. 2002); The ATP hydrolysis and phosphate release steps control the time course of force development in rabbit skeletal muscle (Sleep et al., 2005). At physiological temperatures the ATPase rates of shortening myofibrils from the slow soleus muscle and the fast psoas muscle are similar (Candau et al., 2003).

Such biochemical and physiological informations are needed for the X-ray crystallographers to correlate the structural data with the crossbridge cycle (Geeves and Holmes, 2005). The review of Geeves and Holmes is a unique learning experience. There are three primary conformations of the myosin crossbridge (S1) that can be associated

with states in the Lymn-Taylor (1971) cycle: 1) post-rigor structure where the crossbridge is detached from the actin filament and myosin contains bound ATP (M.ATP); 2) the pre-powerstroke structure where the crossbridge approaches the actin filament and myosin contains the product complex (M.ADP.P_i). 3) rigor-like structure where the crossbridge is attached (in a tilted position) to the actin filament and myosin is combined with actin. In these three conformations, the structures of the crossbridge have deduced from X-ray data of chicken skeletal S1, dictyostelium myosin S1, and skeletal scallop myosin S1. These proteins were crystallized in truncated form (e.g. removing the lever arm), without, and with bound nucleotide. The comparison of these structures leads to the identification of the following conformationally flexible elements: (a) the position of the converter domain; (b) the kink in the relay helix; (c) the positions of SW1 and SW2; (d) the status of the actin binding cleft: open, half open, or shut; (e) the position of the P-loop; (f) the degree of twist of the central β -sheet.

For instance in a comparison of states:

	Rigor (AM)	Post-rigor (M.ATP)
SW1	Open	Closed
Outer Cleft	Shut	Open
Inner Cleft	Closed	Open
SW2	Closed	Open
β -sheet	Maximum twist	No-twist
P-loop	Up	Down
Relay Helix	Straight	Straight
Converter-Lever	Down	Down

In general the review aims to show how structural, biochemical, and mechanical evidence can be used to provide an outline of how actin binding, P_i release, and the powerstroke may be coupled. The review also realizes that work on S1, a soluble fragment of the myosin molecule, may not be extrapolated to intact muscle to understand the molecular mechanism of muscle contraction. Since S1 is no longer attached to the myosin thick filaments, myosin S1 can not be an adequate model for the strained crossbridge (Geeves and Holmes, 2005).

Studies on the Actin-Myosin Interaction in Muscle with X-ray Diffraction and Electron microscopy

Because of its striation, skeletal muscle behaves like a diffraction grating with lines spaced apart at a regular interval equal to the sarcomere length, S. Fig. AM2 illustrates the scheme, from which the basis of diffraction may be understood.

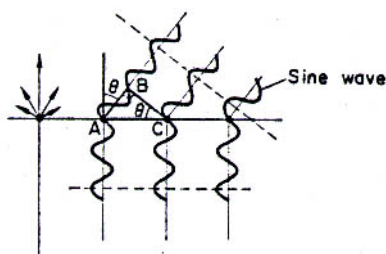


Fig. AM2. Theory of X-ray diffraction of muscle (From Wilkie, 1968).

Points A and C represent the Z lines, thus $AC = S$, the sarcomere length. As the sine waves reach the points A and C they can be regarded as a new light source, scattering light in all directions. Along some directions the scattered waves will be in phase, so the waves reinforce one another and the light is bright. The condition for the first bright fringe is that the path difference AB should be one full wavelength of the light. Thus $AB = \lambda$. Then from the triangle ABC, $\sin \theta = \lambda/S$. The wavelength, λ , is known, the angle, θ , can be experimentally measured and S can be calculated.

As one can measure sarcomere length with the diffraction method, one can also measure the length of the thick and thin filaments.

Hugh Huxley pioneered in obtaining X-ray diffraction pictures from live frog sartorius muscle (Huxley and Brown, 1967, Huxley, 1968), one of his earliest results are shown on Fig. AM3. The longitudinal (meridional) dots arise from the myosin filaments and the horizontal (equatorial) lines from the crossbridges. The numbers represent the reflection of the X-ray beam from the ultrastructure. (The white rectangle in the center and the diagonal line are artifacts). Fig. AM4 shows the model deduced from the X-ray diagram. The diffraction pattern of layer-line reflections corresponds to a repeat of 429 Å and arises from the helical arrangement of crossbridges on the myosin filaments. There are pairs of crossbridges on either side of the thick filaments at 143 Å intervals, with each pair rotated by 120° with respect to each neighbor.

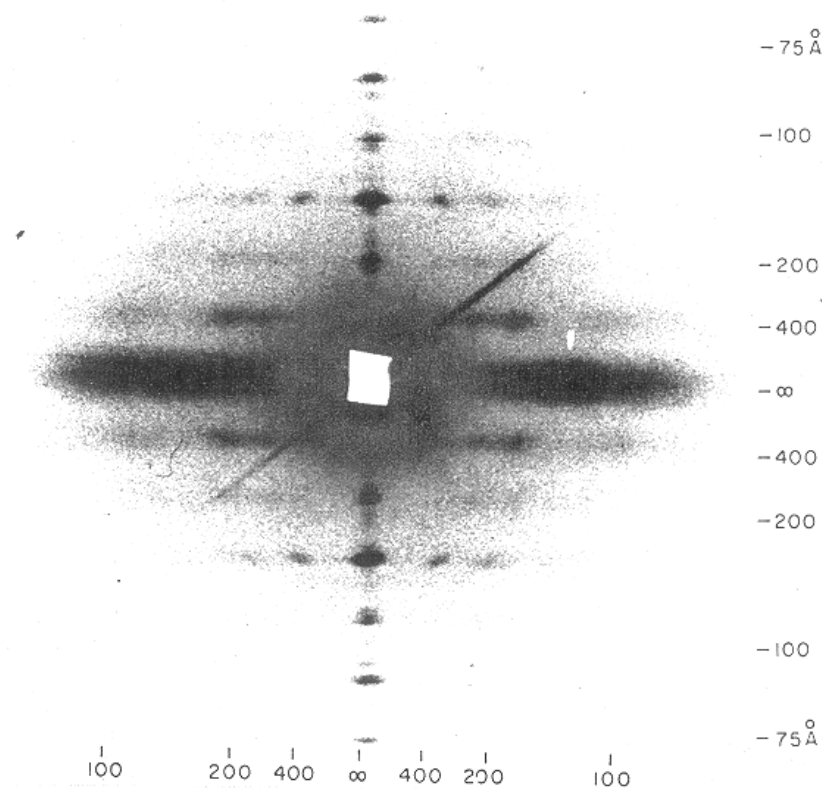


Fig. AM3. X-ray diffraction pattern of live frog muscle (From Wilkie, 1968).

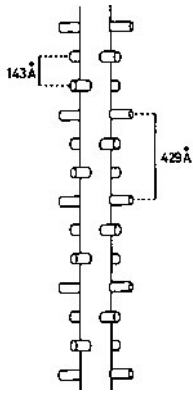


Fig. AM4. Schematic diagram for arrangement of crossbridges in X-ray diagram of frog muscle (From Needham, 1971).

Fig. AM5 compares the equatorial X-ray patterns from live resting frog muscle with muscle in rigor. Note the changes in the intensities of the 1,0 and 1,1 crystallographic directions. In the resting muscle most of the intensity is in 1,0 and only very little in 1,1, whereas in the rigor muscle the intensity of 1,1 is increased greatly. This is explained by the separate entities of myosin and actin filaments in the resting muscle, whereas in the rigor muscle a large part of the myosin heads are attached to actin.

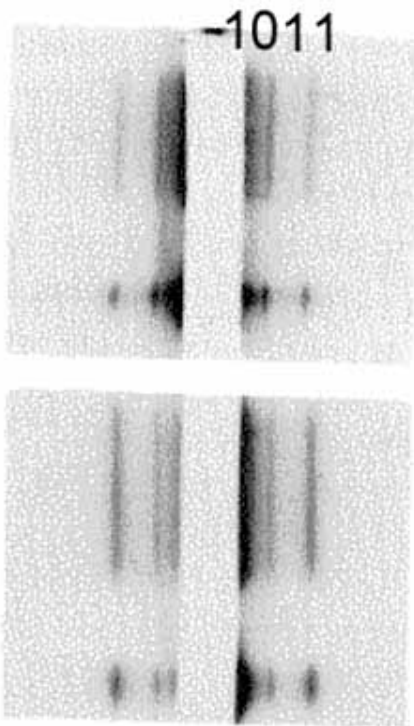


Fig. AM5. Low-angle equatorial X-ray patterns from rabbit psoas muscle: (*top*) live; (*bottom*) in rigor. The pattern shows the 1,0 and 1,1 reflections from the hexagonal lattice of myosin and actin filaments (Reprinted from J. Mol. Biol., vol 37, Huxley, H.E. “Structural difference between resting and rigor muscle; evidence from intensity changes in the low-angle equatorial X-ray diagram”, pp 507-520, 1968, by permission of the publisher, Academic Press).

Toh et al., (2006) reported the first X-ray diffraction study of cardiac myosin crossbridges in mouse heart in the living body. The ratio of the intensities of the equatorial (1,0) and (1,1) reflections decreased from 2.1 in diastole to 0.8 in systole. Stimulation of the β -adrenergic receptor accelerated the decrease in the intensity ratio. The mass transfer to the thin filaments at systole in a β -stimulated heart was close to the

peak value in twitch of frog skeletal muscle indicating that the majority of the crossbridges in the heart were recruited and only a few remained in reserve.

Rapid freezing electron microscopy detected structural changes in the crossbridges accompanying force generation (Hirose et al., 1994). The structure changed dramatically between relaxed, rigor, and with time after initiating contraction. The results supported the models of muscle contraction that have attributed force generation to structural changes in attached crossbridges. With further development of the technique, three-dimensional electron microscope tomography was able to visualize directly motor actions of myosin during contraction of insect flight muscle (Taylor et al., 1999).

In Vitro Motility Assay

Sheetz and Spudich (1983) have introduced the in vitro motility assay for studying actin-myosin interaction at the molecular level. In the motility assay either myosin-coated fluorescent beads are observed moving unidirectional along organized actin filament arrays or single fluorescent-labeled actin filaments are visualized moving over a myosin-coated surface. Movement is initiated by the addition of ATP.

Experiments with the motility assay have shown that myosin determines the actin filament velocity: Pure populations and mixtures of fast skeletal myosin, V1 and V3 cardiac myosin, phosphorylated and un-phosphorylated smooth muscle myosin were studied and the movement of fluorescent-labeled actin filaments over myosin coated surfaces was observed. The actin filament velocities were proportional to the actin-activated ATPase activities of the myosins.

An “optical tweezers” technique (Fig. AM6) was developed in Spudich’s laboratory to measure both the force and step size of single myosin molecules (Finer et al., 1994). Single force transients of 3-4 pN were obtained for movement of 11 nm.

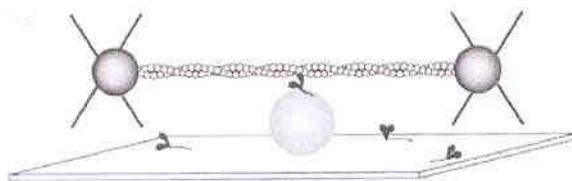


Fig. AM6. Illustration of two optical traps that are focused on beads attached to a single actin filament, which is held near a single heavy meromyosin (HMM) molecule. The filament is pulled taut and lowered onto a silica bead that is firmly fixed to a microscope coverslip and sparsely coated with HMM (From Finer et al., reproduced with permission from Nature, 368, 113-119, 1994, <http://www.nature.com>).

The optical tweezers technique was further improved and used for mapping the actin filament with myosin (Steffen et al., 2001).

Suggested readings: Manstein (2004); Geeves and Holmes (2005).

References

Borejdo, J., Shepard, A., Akopova, I., Grudzinski, W., and Malicka, J. (2004). Rotation of the lever arm of myosin in contracting skeletal muscle fiber measured by two-photon anisotropy. *Biophys J.* **87**, 3912-3921.

Candau, R., Iorga, B., Travers, F., Barman, T., and Lionne, C. (2003). At physiological temperatures the ATPase rates of shortening soleus and psoas myofibrils are similar. *Biophys. J.*, **85**, 3132-3141.

Conibear, P.B., Bagshaw, C.R., Fajer, P.G., Kovács, M., Málnási-Csizmadia, A. (2003). Myosin cleft movement and its coupling to actomyosin dissociation. *Nature Structural Biology*, **10**, 831-835.

Dominguez, R., Freyzon, Y., Trybus, K.M., and Cohen, C. (1998). Crystal structure of vertebrate smooth muscle myosin motor domain and its complex with the essential light chain: visualization of the pre-power stroke state. *Cell*, **94**, 559-571.

Finer, J.T., Simmons, R.M., and Spudich, J.A. (1994). Single myosin molecule mechanics: piconewton force and nanometre steps. *Nature*, **368**, 113-119.

Furch, M., Remmel, B., Geeves, M.A., and Manstein, D.J. (2000). Stabilization of the actomyosin complex by negative charges on myosin. *Biochemistry*, **39**, 11602-11608.

Geeves, M.A., and Holmes, K.C. (1999). Structural mechanism of muscle contraction. *Annu. Rev. Biochem.*, **68**, 687-728.

Geeves, M.A., and Holmes, K.C. (2005). The molecular mechanism of muscle contraction. In *Advances in Protein Chemistry. Fibrous Proteins: Muscle and Molecular Motors*, vol. 71 (J.M. Squire and D.A.D. Parry, eds.), pp 161 – 193, Academic Press, San Diego.

Highsmith, S. (1999). Lever arm model for force generation by actin-myosin-ATP. *Biochemistry*, **38**, 791-797.

Hirose, K., Franzini-Armstrong, C., Goldman, Y.E., and Murray, J.M. (1994). Structural changes in muscle crossbridges accompanying force generation. *J. Cell. Biol.*, **127**, 763-768.

Huxley, H.E. (1968). Structural difference between resting and rigor muscle; evidence from intensity changes in the low-angle equatorial X-ray diagram. *J. Mol. Biol.*, **37**, 507-520.

Huxley, H.E., and Brown, W. (1967). The low angle X-ray diagram of vertebrate striated muscle and its behavior during contraction and rigor. *J. Mol. Biol.* **30**, 383-434.

Lionne, C., Iorga, B., Candau, R., Piroddi, N., Webb, M. R., Belus, A., Travers, F., and Barman, T. (2002). Evidence that phosphate release is the rate limiting step on the overall

- ATPase of psoas myofibrils prevented from shortening by chemical cross-linking. *Biochemistry*, **41**, 13297-13308.
- Lymn, R.W., and Taylor, E.W. (1971). Mechanism of adenosine triphosphate hydrolysis by actomyosin. *Biochemistry*, **10**, 4617-4624..
- Manstein, D. J. (2004). Molecular engineering of myosin. *Philos. Trans. R. Soc. Lond. B Biol. Sci.*, **359**, 1907-1912.
- Needham, D.M. (1971). *Machina Carnis*. Cambridge University Press.
- Rayment, I., and Holden, H.M. (1995). In, *Molecular Aspects of Cell Biology* (R.H. Garrett and C.M. Grisham Eds), Saunders College Publishing.
- Reubold, T.F., Eschenburg, S., Becker, A., Kull, F.J. and Manstein, D.J. (2003). A structural model for actin-induced nucleotide release in myosin. *Nature Structural Biology*, **10**, 826-830.
- Root, D.D., Stewart, S., and Xu, J. (2002). Dynamic docking of myosin and actin observed with resonance energy transfer. *Biochemistry*, **41**, 1786-1794.
- Sheetz, M.P., and Spudich, J.A. (1983). Movement of myosin-coated fluorescent beads on actin cables in vitro. *Nature*, **303**, 31-35.
- Sleep, J., Irving, M., and Burton, K. (2005). The ATP hydrolysis and phosphate release steps control the time course of force development in rabbit skeletal muscle. *J. Physiol.* **563.3**, 671-687.
- Steffen, W., Smith, D., Simons, R., and Sleep, J. (2001). Mapping the actin filament with myosin. *Proc. Natl. Acad. Sci. USA*, **98**, 14949-14954.
- Taylor, K.A., Schmitz, H., Reedy, M.C., Goldman, Y.E., Franzini-Armstrong, C., Sasaki, H., Tregear, R.T., Poole, K., Lucaveche, C., Edwards, R.J., Chen, L.F., Winkler, H., and Reedy, M.K. (1999). Tomographic 3D reconstruction of quick frozen, Ca²⁺-activated contracting insect flight muscle. *Cell*, **99**, 421-431.
- Toh, R., Shinohara, M., Takaya, T., Yamashita, T., Masuda, S., Kawashima, S., Yokoyama, M., and Yagi, N. (2006), An x-ray diffraction study on mouse cardiac crossbridge function in vivo: effects of adrenergic β -stimulation. *Biophys. J.*, **90**, 1723-1728.
- Wilkie, D.R. (1968). *Muscle*. St. Martin Press.
- Zeng, W., Conibear, P.B., Dickens, J.L., Cowie, R.A., Wakelin, S., Málnási-Csizmadia, A., and Bagshaw, C.R. (2004). Dynamics of actomyosin interactions in relation to the crossbridge cycle. *Phil. Trans. R. Soc. B.*, **359**, 1843-1855.